Alkylation and Cross-Linking of DNA by the Unnatural Enantiomer of Mitomycin C: Mechanism of the DNA-Sequence Specificity of Mitomycins

Dario Gargiulo,[1a] Stephen S. Musser,[1b] Lihu Yang,[1c] Tohru Fukuyama,[1c] and Maria Tomasz*,[1a]

Contribution from the Department of Chemistry, Hunter College, City University of New York, New York, New York 10021, Instrumentation and Biophysics Branch, U.S. Food and Drug Administration, 200 C Street, S.W., Washington, D.C. 20204, and Department of Chemistry, Rice University, Houston, Texas 77005-1892

Received April 25, 1995[⊗]

Abstract: The unnatural enantiomer (*ent*) of the antitumor antibiotic mitomycin C (MC) forms both a mono- and a bisguanine adduct in DNA upon reductive activation, with the bisadduct constituting DNA interstrand cross-links. The structures of the two adducts were rigorously determined using less than 1 mg of available material. The adducts are diastereomers of the known major guanine adducts of natural MC: the 2″-NH_2 group is in the α- instead of the β-configuration while the chirality of the 1″-linkage to DNA guanine is α, as with natural MC. The extent of DNA adduct formation was 20−50% of that of MC. Enzymatic reductive activation of both MC and *ent*-MC by NADPH−cytochrome *c* reductase proceeded at equal rates. Both the monoalkylation and the cross-linking reactions of *ent*-MC exhibited DNA-sequence selectivity for the CpG sequence in analogy to that by natural MC. This finding indicates that at this sequence activated MC and *ent*-MC both assume preferentially the "carbamate upstream" orientation along the DNA minor groove with respect to the target guanine, which exposes the prochiral C1″-center of these drugs to a α-stereofacial attack by DNA guanine N^2. The results also reinforce the earlier proposal that prior to the covalent step a simple, common structural element, i.e., the 10″-carbamate group, recognizes the CpG sequence by formation of a specific H-bond, and this enhances the rate of alkylation of the guanine at the CpG site. It is proposed that the fit of the 1″,2″-*cis*-substituted adducts resulting from *ent*-MC in the minor groove is not as favorable as that of the 1″,2″-*trans*-adducts of natural MC, and that this is the reason for the observed lower reactivity of *ent*-MC with DNA, as compared with MC. This lower reactivity to form DNA adducts may be the basis for the slightly (approximately 50%) lower cytotoxicity of *ent*-MC than of MC to tumor cells.

The study of interactions of DNA with ligands of differing chiralities provides a rich ground for applications to mechanisms of molecular recognition, probing of polymorphism of DNA, and structure−biological activity correlations. Comparing the DNA-interaction chemistry between individual members of enantiomeric or diastereomeric pairs of chiral metal complexes,[2] antitumor agents, and carcinogens has provided sharp insights into such phenomena. Recent notable examples are the alkylation of DNA by the stereoisomers of the carcinogenic benzo[*a*]pyrenediol epoxides (BPDE),[3,4] the natural and unnatural enantiomers of CC-1065,[5a] and enantiomeric pairs of CC-1065 functional derivatives[5b] and of duocarmycin SA,[5c] as well as the enantiospecific recognition of DNA for cleavage by bleomycin.[6] NMR studies of the DNA adducts of the BPDE enantiomers (+)- and (−)-*anti*-BPDE revealed an extraordinary relationship among the stereochemistry of the drug−DNA linkage, adduct orientation in the minor groove, and tumorigenicity.[7] The two enantiomers of CC-1065 were shown to be potent cytotoxins, which however displayed distinct DNA-sequence selectivities and opposite groove orientation of the adducts.[5a]

Chart 1

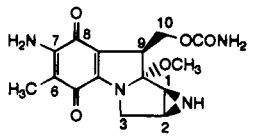

1 (MC)

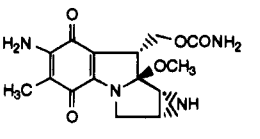

2 (*ent*-MC)

Our goal was to compare the interactions of another enantiomeric pair of DNA-reactive agents with DNA: the natural antitumor antibiotic mitomycin C (MC;[3] **1**) and its unnatural enantiomer, *ent*-MC (**2**) (Chart 1). The latter has been obtained recently by the resolution of fully synthetic racemic MC,[8]

[⊗] Abstract published in *Advance ACS Abstracts*, September 1, 1995.

(1) (a) Hunter College. (b) U.S. Food and Drug administration. (c) Rice University.

(2) Barton, J. K. *Science* **1986**, *233*, 727−734.

(3) Abbreviations: BPDE, benzo[*a*]pyrenediol epoxide; MC, mitomycin C; *ent*, enantiomeric; *ent*-MC, enantiomer of natural MC; m^5C, 5-methylcytosine; TEAA, triethylammonium acetate; SVD, snake venom diasterase; *E*, molar extinction coefficient.

(4) Geacintov, N. E. In *Polycyclic Aromatic Hydrocarbon Carcinogenesis: Structure-Activity Relationships*; Yang, s. K., Silverman, B. D., Eds.; CRC: Boca Raton, FL, 1988; Vol. 2, pp 181−206.

(5) (a) Hurley, L. A.; Warpehoski, M. A.; Lee, C.-S.; McGovern, J. P.; Scahill, T. A.; Kelly, R. C.; Mitchell, M. A.; Wicniewski, N. A.; Gebhard, I.; Johnson, P. D.; Bradford, S. *J. Am. Chem. Soc.* **1990**, *112*, 4633−4649. (b) Boger, D. L.; Coleman, R. S.; Invergo, B. J.; Sakya, S. M.; Ishizaki, T.; Munk, S. A.; Zarrinmayeh, H.; Kitos, P. A.; Thompson, S. C. *J. Am. Chem. Soc.* **1990**, *112*, 4623−4632. (c) Boger, D. L.; Johnson, D. S.; Yun, W. *J. Am. Chem. Soc.* **1994**, *116*, 1635−1656.

(6) Urata, H.; Ueda, Y.; Usami, Y.; Akagi, M. *J. Am. Chem. Soc.* **1993**, *115*, 7135−7138.

(7) (a) de los Santos, C.; Cosman, M.; Hingerty, B. E.; Ibanez, V.; Margulis, L. A.; Geacintov, N. E.; Broyde, S.; Patel, D. J. *Biochemistry* **1992**, *31*, 5245−5252. (b) Cosman, M.; de los Santos, C.; Fiala, R.; Hingerty, B. E.; Ibanez, V.; Luna, E.; Harvey, R.; Geacintov, N. E.; Broyde, S.; Patel, D. J. *Biochemistry* **1993**, 4145−4154.

(8) Yang, L., Ph.D. Thesis, Rice University, Houston, TX, 1990.

(9) Fukuyama, T.; Yang, L. *J. Am. Chem. Soc.* **1987**, *109*, 7881−7882.

0002-7863/95/1517-9388$09.00/0

Scheme 1. Structures of Mitomycin C–DNA Adducts Obtained under Monofunctional and Bifunctional Activating Conditions

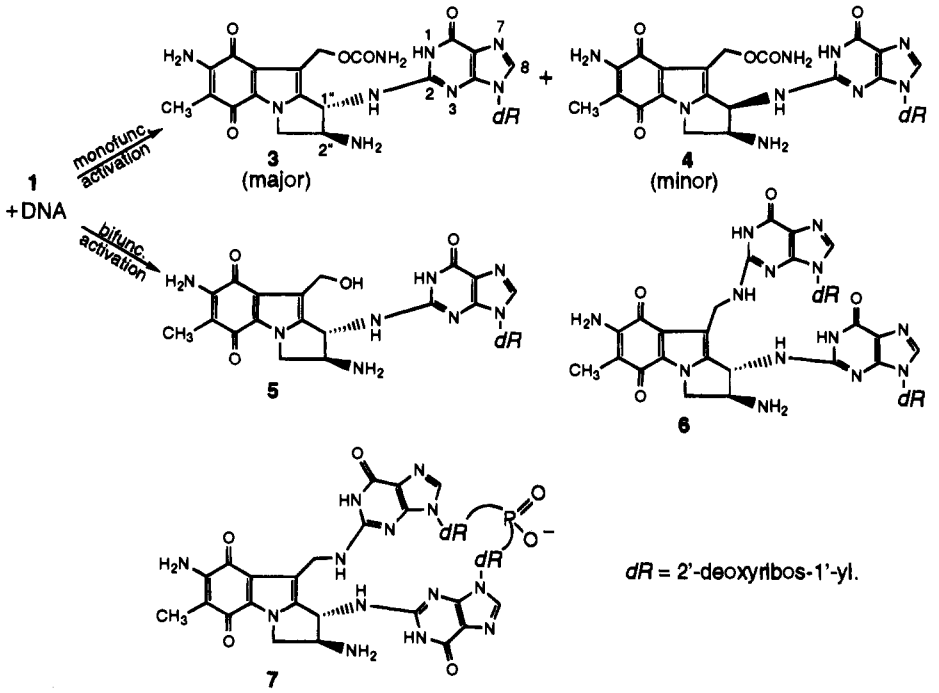

synthesized by Fukuyama and co-workers.[9] MC, which is used clinically as a cancer chemotherapeutic agent, alkylates and cross-links DNA. This property is most likely to constitute the molecular basis of the cytotoxic and antitumor activity of the mitomycins.[10] The major MC–DNA adducts formed in cell-free systems were previously isolated and structurally elucidated (Scheme 1).[11] The structures indicated that the sole sites of alkylation by MC are the N^2 atoms of guanines, in the minor groove of DNA. Reductive activation of MC is required for the DNA-alkylation process.[10] The first, monofunctional alkylation step leads to monoadduct **3**; under the conditions of bifunctional activation this is followed by a second alkylation step to bisadduct **6** which constitutes a DNA interstrand cross-link[12] or, less frequently, an intrastrand cross-link (**7**).[11d] The 10″-decarbamoylated monoadduct **5** is also a major product.[11c] The same adducts were detected and identified *in vivo*.[11b,13]

The solution structures of duplex oligonucleotides containing a MC cross-link (bisadduct **6**)[14] and the major monofunctional MC adduct **3**[15] were determined by 2-D NMR, combined with molecular dynamics computation. The structures revealed that the monoadduct assumes a specific orientation in the minor groove, with its C10″-carbamate function positioned in the 5′-direction from the linked guanine (Figure 1, **A**). This orientation is preserved in the cross-link,[14] formed from the monoadduct when the C10″-carbamate is displaced by the 2-amino group of a second guanine in the opposite strand (CpG•CpG cross-link, Figure 1, **A**). The solution structures[14,15] explain fully the previously observed specificity of the MC cross-link to the CpG•CpG dinucleotide sequence in duplex DNA.[16] They show that, *given this orientation (A)*, the monoadduct can reach a second guanine only at this sequence to form the cross-link. The same monoadduct in the opposite orientation (**B**) could potentially give GpC•GpC cross-links, but such cross-links are not formed with MC (Figure 1). The structural determinant of the specific orientation of the MC monoadduct was proposed to be the chirality of the drug–DNA bond, i.e., the C1″-α-linkage to the N^2 atom of the guanine in adduct **3**.[17]

A potential probe of this hypothesis is determination of the chirality and orientation of the analogous adduct from *ent*-MC, provided such an adduct is formed at all. We report here that *ent*-MC forms covalent mono- and bisadducts with DNA upon reductive activation in a chemical process analogous to that of MC. We found that the chirality of the *ent*-MC–DNA bond of the major monoadduct is the same (α) as that of the MC–

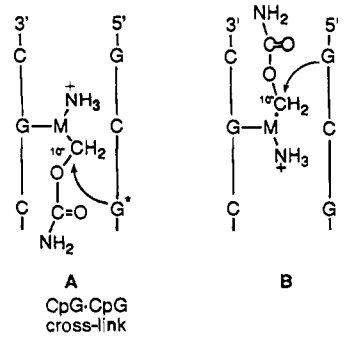

Figure 1. Cross-linking of a mitomycin monoadduct in two opposite orientations.

(10) Szybalski, W.; Iyer, V. N. In *Antibiotics I: Mechanism of action*; Gottlieb, D., Shaw, P. D., Eds.; Springer-Verlag: New York, 1967; pp 230–245.

(11) (a) Tomasz, M.; Chowdary, C.; Lipman, R.; Shimotakahara, S.; Veiro, D.; Walker, V.; Veridine, G. L. *Proc. Natl. Acad. Sci. U.S.A.* **1986**, *83*, 6702–6706. (b) Tomasz, M.; Lipman, R.; Chowdary, D.; Pawlak, J.; Verdine, C. L.; Nakanishi, K. *Science* **1987**, *235*, 1204–1208. (c) Tomasz, M.; Lipman, R.; McGuiness, B. F.; Nakanishi, K. *J. Am. Chem. Soc.* **1988**, *110*, 5892–5896. (d) Bizanek, R.; McGuiness, B. F.; Makanishi, K.; Tomasz, M. *Biochemistry* **1992**, *31*, 3084–3091.

(12) Borowy-Borowski, H.; Lipman, R.; Chowdary, D.; Tomasz, M. *Biochemistry* **1990**, *29*, 2992–2999.

(13) Bizanek, R.; Chowdary, D.; Arai, H.; Kasai, M.; Hughes, C. S.; Sartorelli, A. C.; Rockwell, S.; Tomasz, M. *Cancer Res.* **1993**, *53*, 5127–5134.

(14) Norman, D.; Live, D.; Sastry, M.; Lipman, R.; Hingerty, B. E.; Tomasz, M.; Broyde, S.; Patel, D. J. *Biochemistry* **1990**, *29*, 2861–2876.

(15) Sastry, M.; Fiala, R.; Lipman, R.; Tomasz, M.; Patel, D. J. *J. Mol. Biol.* **1995**, *247*, 338–359.

(16) (a) Teng, S. P.; Woodson, S. A.; Crothers, D. M. *Biochemistry* **1989**, *28*, 3901–3907. (b) Weidner, M. F.; Millard, J. T.; Hopkins, P. B. *J. Am. Chem. Soc.* **1989**, *111*, 9270–9272. (c) Borowy-Borowski, H.; Lipman, R.; Tomasz, M. *Biochemistry* **1990**, *29*, 2999–3006.

(17) Millard, J. T.; Weidner, M. F.; Raucher, S.; Hopkins, P. B. *J. Am. Chem. Soc.* **1990**, *112*, 3637–3641.

(18) (a) Li, V.; Kohn, H. *J. Am. Chem. Soc.* **1991**, *113*, 275–283. (b) Kumar, S.; Lipman, R.; Tomasz, M. *Biochemistry* **1992**, *31*, 1399–1407. (c) Kohn, H.; Li, V.; Tang, M.-S. *J. Am. Chem. Soc.* **1992**, *114*, 5501–5509.

Scheme 2. Intermediates in the Reductive Activation of MC and *ent*-MC[a]

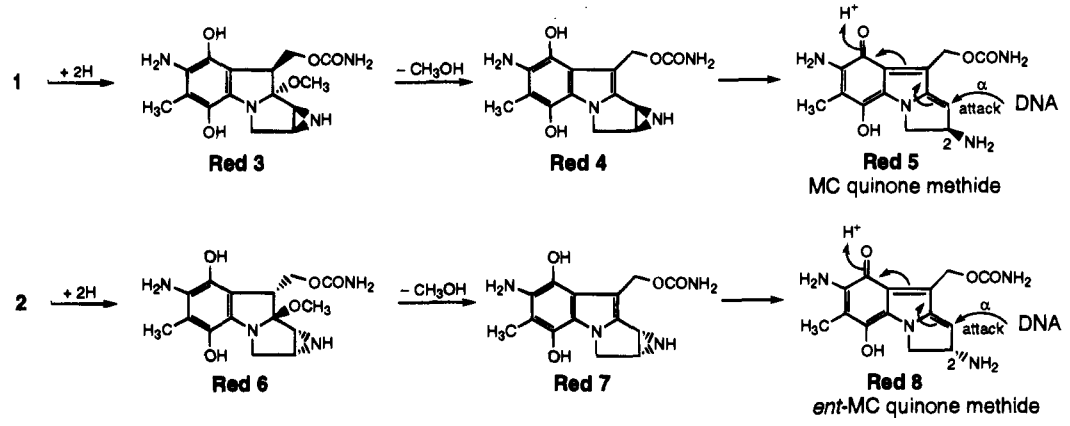

[a] The prefix **Red** indicates the reduced nature of the compounds.

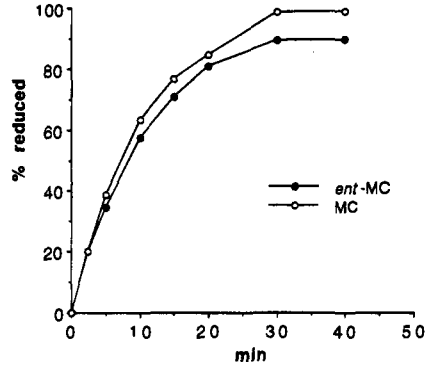

Figure 2. Kinetic plots of the reduction of *ent*-MC (●) and MC (○) by NADPH−cytochrome *c* reductase/NADPH.

DNA bond of the major natural MC monoadduct, despite the opposite configuration of the aziridines of MC and *ent*-MC. The orientation of the *ent*-MC adduct in the minor groove was also determined and was shown to be the same as that of the MC adduct. These results demonstrate that, indeed, the observed specific orientation of the mitomycin monoadduct (Figure 1, **A**) is intrinsically associated with the α-chirality of the mitomycin linkage to DNA, as predicted by Hopkins and coworkers.[17] It is also concluded from the findings that this orientation is assumed by both enantiomers *prior* to covalent bond formation, in a sequence-selective manner. The chirality of the oriented noncovalent drug−DNA complexes disposes both mitomycins for an α-stereofacial attack by the DNA guanine.

An added impetus for the present study was the finding that *ent*-MC exhibited *in vitro* antitumor activity.[19] We found that *ent*-MC alkylated and cross-linked DNA less efficiently than MC, and this appears to correlate with its slightly lower cytotoxicity to tumor cells.[19]

Results

Enzymatic Reduction of MC and *ent*-MC. To test whether *ent*-MC is a substrate for NADPH−cytochrome *c* reductase, a flavoenzyme important in the reductive activation of MC *in vivo*,[20] a kinetic reduction study was conducted of both mitomycins in which the rate of disappearance of the starting material was monitored by HPLC. The results (Figure 2) show that both are converted to new products as a result of the enzymatic reduction of the quinone, at the same rate. This indicates that the reduction itself (the single enzymatic step in the multistep activation cascade; Scheme 2) proceeds at the same rate for both enantiomers.

Cross-Linking of DNA by MC and *ent*-MC. ^{32}P-end-labeled linear pBR322 DNA was submitted to reductive cross-linking by both enantiomers employing $Na_2S_2O_4$ under anaerobic conditions. The yield of cross-linked DNA was determined by a gel electrophoretic assay.[21] Figure 3 illustrates that both enantiomers cross-link DNA, but *ent*-MC is less efficient at all drug concentrations employed. At 10 and 20 μM drug concentrations 3.6- and 2.1-fold less cross-linking occurs with *ent*-MC; the difference decreases as cross-linking approaches saturation.

Cross-Linking of Synthetic Oligonucleotides by MC and *ent*-MC. 16a in the self-complementary duplex form was treated with *ent*-MC or MC under bifunctional MC-activating conditions which employed drug reduction by $Na_2S_2O_4$ under argon,[12] similarly to that in the above experiment. HPLC of the reaction mixture indicated that duplex **16a** was cross-linked by *ent*-MC and MC. This was inferred from the appearance of a peak (marked **18** and **19**, Figure 4a,b, respectively) eluting later than that of the unmodified starting material, which, in the case of MC, was previously shown to be the cross-linked oligonucleotide **19**.[12] No cross-linking occurred by either enantiomer using another oligonucleotide, **25a**, in which the central CpG step was replaced by a GpC step (Figure 4c).

Adduct Formation of *ent*-MC with *Micrococcus luteus* DNA and Synthetic Oligonucleotides. (i) Under bifunctional MC-activation conditions which employed drug reduction by $Na_2S_2O_4$ under argon,[11b,12] *ent*-MC formed a product with DNA as seen by HPLC of the nuclease digest of the drug-treated DNA (Figure 5b, peak marked **9**) which had a greater retention time than that of the known MC bisadduct **6** formed under the same conditions (Figure 5a). The synthetic oligonucleotide **16a** yielded the same pair of adducts: **6** from MC and **9** (Chart 2) from *ent*-MC (Figure 6a,b, respectively).

(ii) Under monofunctional activation conditions (H_2/PtO_2 reducing agent),[11a] *ent*-MC alkylated the oligonucleotides **16a**, **16b**, and **17** (Chart 3). This was seen upon HPLC of the nuclease digests of the drug-treated oligonucleotides (Figure 7b). The late-eluting peak marked **8** was assumed to be a major adduct of *ent*-MC which was different from the known major MC adduct **3**, formed between MC and oligonucleotide **17** under the same conditions (Figure 7a).

Isolation of Adducts of *ent*-MC from Nuclease Digests of ***ent*-MC−Oligonucleotide Complexes.** Both adducts **8** and **9** were isolated from the digests, using HPLC and collecting the

(19) K. Gomi, Kyowa Hakko Kogyo Co., Tokyo, Japan, personal communication.

(20) Keyes, S. R.; Fracasso, P. M.; Heimbrooks, D. C.; Rockwell, S.; Sligar, S. G.; Sartorelli, A. C. *Cancer Res.* **1984**, *44*, 5638−5643.

(21) Hartley, J.; Berardini, M. D.; Souhami, R. L. *Anal. Biochem.* **1991**, *193*, 131−134.

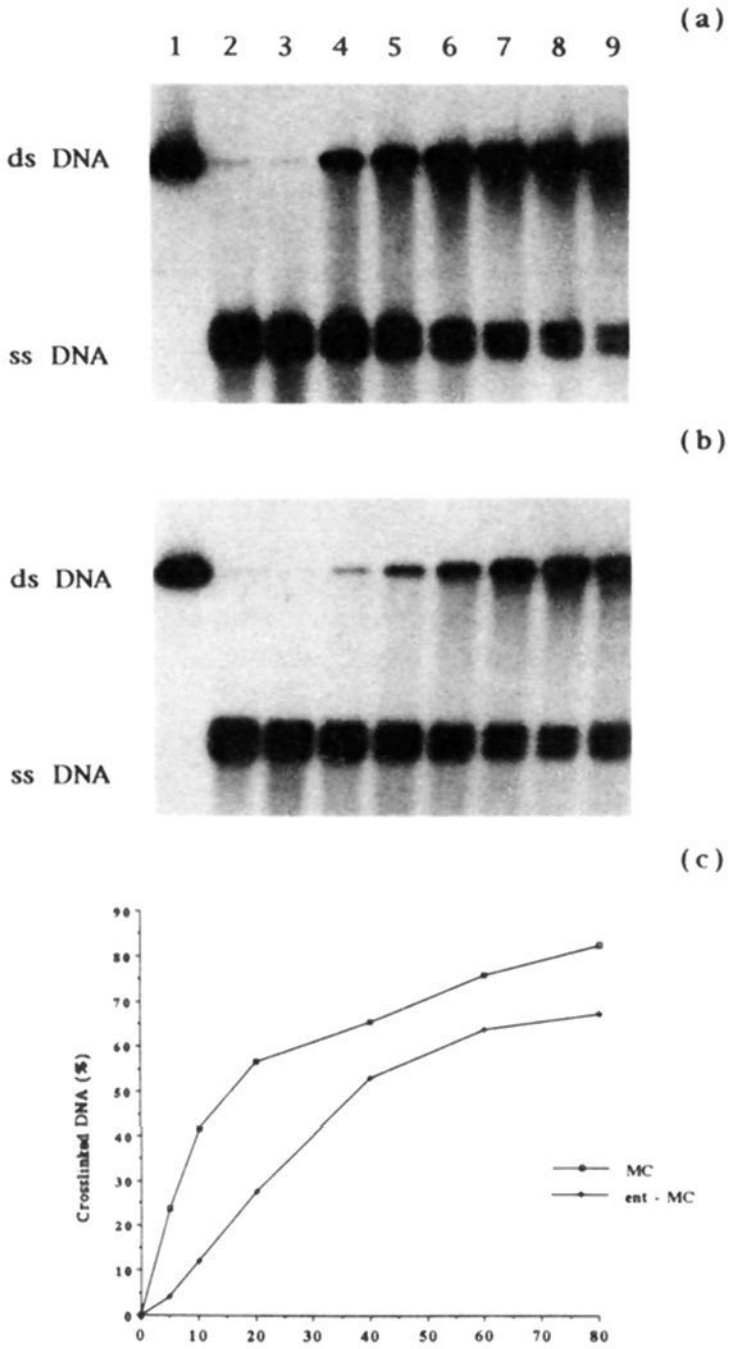

Figure 3. Comparison of cross-linking efficiency of *ent*-MC and MC under activation by $Na_2S_2O_4$. (a) Autoradiograph of an agarose gel showing cross-linking of ^{32}P-pBR322 DNA by MC. Complete system: 118 μM DNA was treated with varying amounts of MC and 1.2 mM $Na_2S_2O_4$ at room temperature for 1 h under anaerobic conditions, followed by heat denaturation as described in Methods. Lanes 1−9 contained the following: (a) control linear ^{32}P-pBR322 DNA; (2) same, heat-denatured; (3−9) complete system; MC concentrations are 0, 5, 10, 20, 40, 60, and 80 μM, respectively. (b) Cross-linking by *ent*-MC. Complete system was the same as in (a), using *ent*-MC instead of MC. (c) Percent cross-linking as a function of drug concentration, measured by densitometry of the autoradiogram of the gels for MC and *ent*-MC.

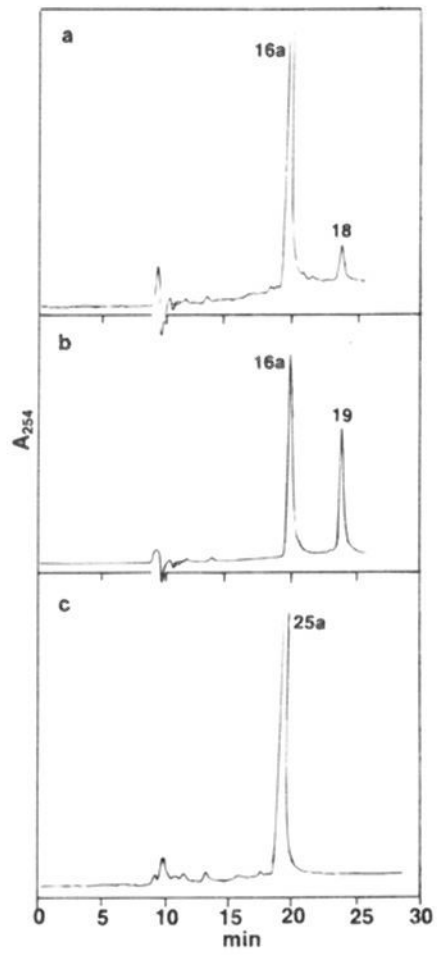

Figure 4. Cross-linking of oligonucleotides by *ent*-MC under reductive activation: HPLC of the reaction mixture. (a) Oligonaucleotide **16a** was cross-linked by *ent*-MC upon bifunctional activation by $Na_2S_2O_4$, in 7% yield. (b) In a comparative experiment, MC was shown to cross-link **16a** in 38% yield. (c) *ent*-MC does not cross-link oligonucleotide **25a** under the same reductive activation conditions by $Na_2S_2O_4$. HPLC conditions: Rainin Dynamax-300 C-4 column (10 mm × 25 cm); 9−19.5% CH_3CN in 0.1 M TEAA, pH 7.0, in 40 min; flow rate 2.0 mL/min.

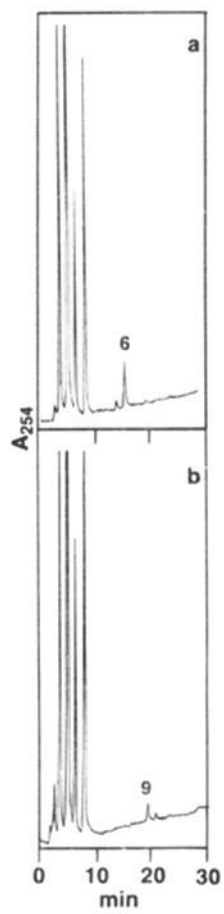

Figure 5. *M. luteus* DNA cross-link adducts: HPLC of digests. (a) Digest of the MC−DNA complex. (b) Digest of the *ent*-MC−DNA complex. HPLC conditions: reversed-phase C-18 column (Beckman Ultrasphere ODS), 0.4 × 25 cm; 6−18% CH_3CN in 0.02 M NH_4AC, pH 5.2, in 30 min; flow rate 1 mL/min.

appropriate peaks indicated in Figures 7b and 6b, respectively. Approximately 0.8 μmol of **8** and 0.3 μmol of **9** were accumulated over the course of this work from 8 mg (23 μmol) of *ent*-MC.

Determination of the Structure of *ent*-MC Monoadduct 8. The UV spectrum of **8** was identical to that of authentic **3**[11a] and very similar to that of **4**,[11c] indicating that it, too, is a mitosene−deoxyguanosine adduct. The electrospray ionization mass spectrum (ESIMS) confirmed this by exhibiting the expected molecular ion peak at $m/z = 570$ along with several fragments typical of 7-aminomitosene adducts (see Figure 8 and the Experimental Section).

The circular dichroism (CD) spectrum (Figure 9) above 260 nm was *essentially the mirror image of the CD of adduct* ***4***, a known minor adduct of MC. The small broad negative Cotton effect above 500 nm is itself diagnostic of α-stereochemistry of a C1″-substituent in 7-aminomitosenes in general, according to the empirical relationship derived earlier from the CD of a large number of different C1″-substituted mitosene derivatives.[22] From this we hypothesized that **8** was diastereomeric with **3**

(22) Tomasz, M.; Jung, M.; Verdine, G. L.; Nakanishi, K. *J. Am. Chem. Soc.* **1984**, *106*, 7367−7370.

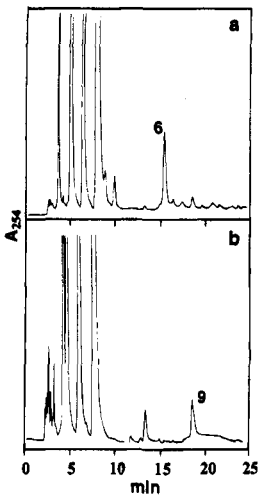

Figure 6. Isolation of the "cross-link" adducts **6** and **9** from digests of cross-linked oligonucleotides: HPLC of digests. (a) Digest of MC–oligonucleotide complex **19**. (b) Digest of *ent*-MC–oligonucleotide complex **20**. HPLC conditions: as in Figure 5.

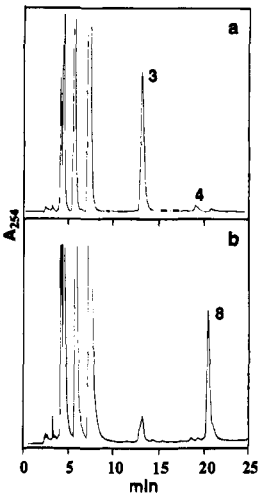

Figure 7. Isolation of monoadducts **3** and **8** from digests of monoadducted oligonucleotides: HPLC of the digests. (a) Digest of MC–oligonucleotide complex **24**. (b) Digest of *ent*-MC–oligonucleotide complex **23**. HPLC conditions: as in Figure 5. The minor peak at 13 min was not identified. It is thought to be the 1"-β-isomer of **8**, as yet unknown.

Chart 2

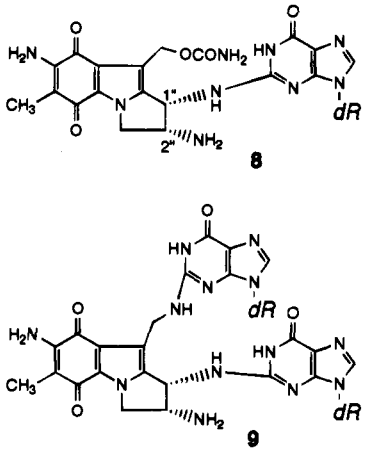

Chart 3

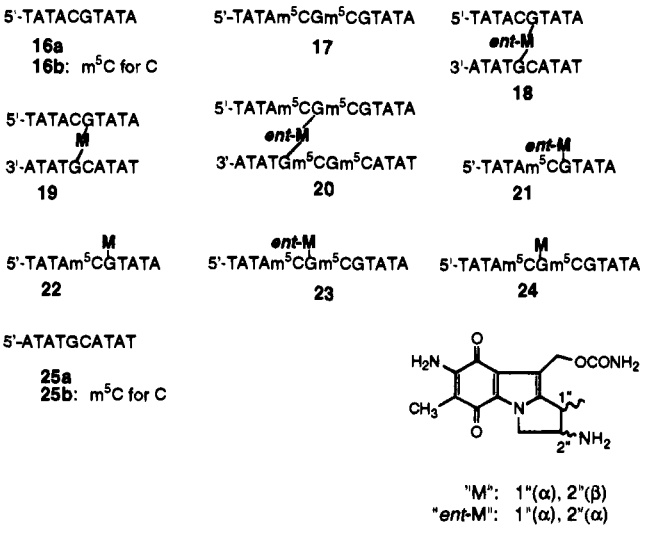

and **4** and its 1",2"-stereochemistry is antipodal to that in **4** (Scheme 3). In order to prove this conclusively, we sought to remove the deoxyribose moiety from both **4** and **8**, reasoning that this would give two *enantiomeric* mitosene–guanine adducts. This was not accomplished however, by acid hydrolysis directly of **4** and **8**, due to the stability of the glycosidic linkage in these mitomycin–dG adducts.[23] However, upon treatment of the set of adducts **3**, **4**, and **8** with $(CH_3)_2SO_4$ (Scheme 3), the resulting N^7-methylguanine derivatives **10**, **11**, and **12** readily lost their deoxyribose under mild acidic conditions,[24] to give N^7-methylguanine–mitosene adducts **13**, **14**, and **15**, respectively (Scheme 3). All of these substances (**10**–**15**) were characterized by UV and ESIMS. Both types of spectra were consistent with the intended transformations (Experimental Section). Conclusive proof that **14** and **15** are indeed enantiomers was provided by their coelution upon HPLC (Figure 11c), identical UV spectra, and mirror image CD spectra (Figure 10). The slight deviations from a perfect mirror image (Figure 10; CD) are attributed to spectral error, considering that extremely dilute solutions (<0.01 absorbance at the 257 nm maximum) were employed, by necessity, for these measurements.

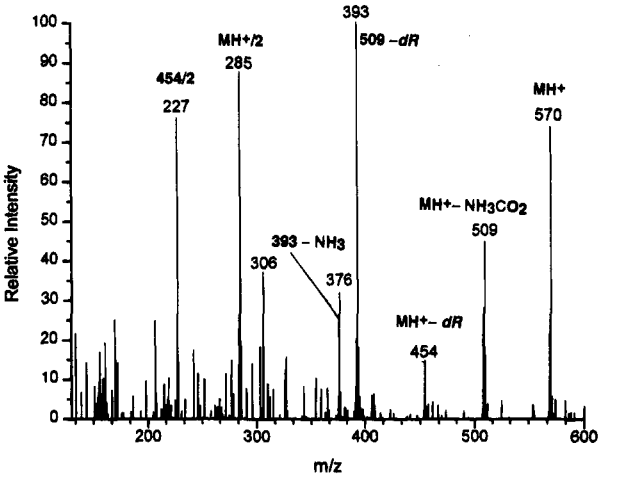

Figure 8. ESIMS of the major *ent*-MC monoadduct **8**.

Proving the enantiomeric relationship of **14** and **15** thus defines the original structural relationship of the *ent*-MC monoadduct **8** to the known MC monoadduct **4** (Scheme 3): **8** is diastereomeric with **4**, having opposite chiralities at both C1" and C2". This in turn fully defines the structure of **8** as shown.

Structure of the *ent*-MC Cross-Link Adduct 9. In contrast to the case of *ent*-MC monoadduct **8**, above, the 1"-β,2"-β-

(23) Tomasz, M.; Lipman, R.; Snyder, J. K.; Nakanishi, K. *J. Am. Chem. Soc.* **1983**, *105*, 2059–2063.

(24) Lawley, P. D.; Brookes, P. *Biochem. J.* **1963**, *89*, 127.

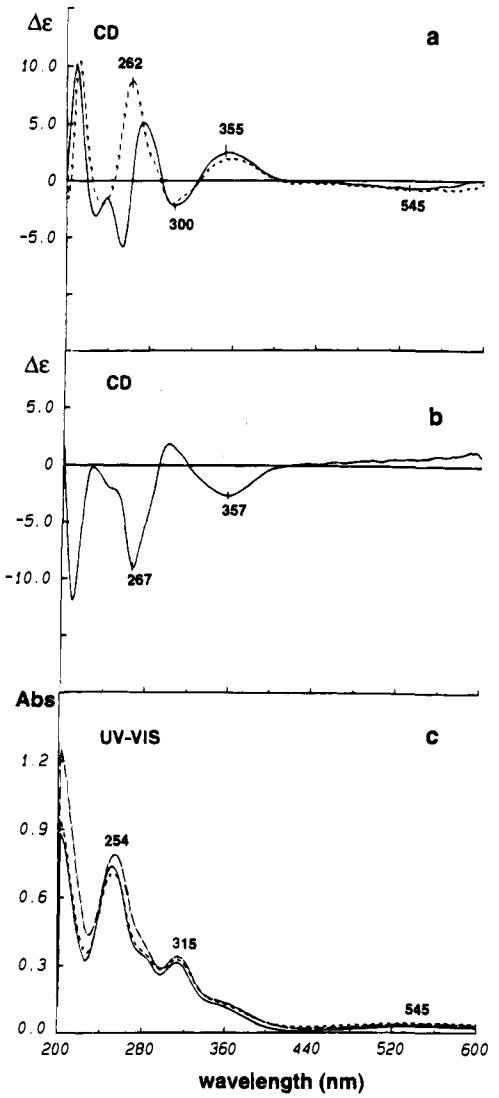

Figure 9. CD and UV−vis spectra in water of monoadducts **3**, **8**, and **4** (Scheme 2). (a) The two major monoadducts obtained from MC and *ent*-MC are shown in solid (**3**) and dashed (**8**) lines, respectively. (b) CD of *cis*-isomer monoadduct **4**, isolated after monoalkylation reaction of MC with oligonucleotides. (c) The UV−vis spectra of monoadducts **3**, **8**, and **4** are shown in solid, dashed, and dashed−dotted lines, respectively.

diastereomer of bisadduct **9** is not known; therefore, a different scheme was employed for identification. The characteristic UV and CD spectra of **9** were very similar to those of the known bisadduct **6** from natural MC[11b] (Figure 12). The broad negative Cotton effect in the 500−600 nm region again indicated C1″-α-stereochemistry[11b] as in **8** above. ESIMS showed a single peak at $m/z = 776$, corresponding to the calculated molecular ion of **9**. As seen in Scheme 4, the monoadduct oligonucleotide **23** (rigorously characterized by enzymatic digestion; see the Experimental Section) was annealed to **17** and treated with $Na_2S_2O_4$. This converted **23** to a *cross-linked oligonucleotide* (**20**) (Figure 13), as verified by obtaining *ent*-MC bisadduct **9** from enzymatic digestion of **20** (Figure 6b). The fact that the proven *ent*-MC monoadduct **8** in its oligonucleotide-bound state (**23**) was converted to **9** upon further reductive activation, together with the ESIMS data, leaves little doubt as to the structure of **9**. The analogous smooth reductive conversion of oligonucleotide-bound monoadduct to bisadduct (**3** to **6**) has been previously demonstrated in the case of natural MC.[16c]

CpG-Sequence Specificity of Monoalkylation by MC and *ent*-MC. Alkylation of Oligonucleotides **16b** by monofunctionally activated MC or *ent*-MC yielded 78% of monoadduct **3** and 25% of monoadduct **8**, respectively (Figure 14a,b). This oligonucleotide has both guanines in the m^5CpGpT sequence context. m^5C was substituted for C since such substitution is known to result in a higher yield of monoalkylation of the guanine than of the guanine at CpGpT.[25] In contrast, oligonucleotide **25b** (guanine in the TpGpm^5C context) gave only very low yields of the respective monoadducts of MC and *ent*-MC (<5% in each case; Figure 14c,d). It is concluded that *ent*-MC shows the same CpG-sequence specificity of monoalkylation as MC.[18]

Sequence Specificity of DNA Cross-Linking by *ent*-MC. Earlier, in the case of natural MC, two prototype self-complementary 10-mer oligonucleotides were compared as substrates for cross-linking: **16a**, presenting a CpG•CpG site, and **25a**, presenting a GpC•GpC site, for interstrand bisadduct formation. MC exhibited complete specificity for the former since it cross-linked **16a** but not **25a**.[16c] The same oligonucleotide pair was now applied to test *ent*-MC. Only **16a** showed cross-linking as seen by comparing parts a and c of Figure 4. Thus, cross-linking by *ent*-MC is apparently specific to CpG•CpG, similarly to that by natural MC.

Comparative Efficiency of DNA Cross-Linking and Formation of Adducts by *ent*-MC and MC. *ent*-MC interacts less efficiently with DNA than MC, in both its cross-linking and monoalkylation activity. This is seen from a comparison of yields of products obtained from the two drugs under identical conditions (Table 1). The cross-link yields of *ent*-MC are only 20%, 28%, and 45% of those of MC in the three sets of data. The yields of monoadduct **8** of *ent*-MC are 32% and 20% of the yields of monoadduct **3** from MC, as seen in the two sets of comparative data.

Mass Spectroscopy. Positive electrospray ionization mass spectroscopy using the LC−MS method proved to be superior to fast atom bombardment (FAB) (positive ion mode) in the analysis of the mitomycin−DNA adducts. Successful analysis of adducts **4**, **8**, **13**, and **15** was carried out by ESIMS as described above and in the Experimental Section individually. The FAB method was successful only in the case of bisadduct **9**. It is notable that mitomycin adducts undergo fragmentation under the conditions of ESIMS as shown in Figure 8, for example. The fragments typically indicate loss of the C10″-carbamate, deoxyribose, and NH_3 in various combinations.

Discussion

The focus of this investigation was a comparison between the known, well-characterized reaction of MC with its biological target DNA and the corresponding reaction of the unnatural enantiomer, *ent*-MC, determined in the present work. Since *ent*-MC was found earlier to be cytotoxic in the tumor cell line tested, displaying half of the potency of MC upon direct comparison (Table 2),[19] it was expected to alkylate DNA but perhaps less intensively than MC or to give less toxic alkylation products. Most of these expectations were fulfilled as follows.

Enzymatic reduction by NADPH−cytochrome *c* reductase/NADPH, a major MC-activating system in tumor cells,[20] was found to be equally efficient for MC and *ent*-MC. This is not surprising in view of the wide structural variety of quinones which are substrates of this enzyme.[26] This rules out differential enzymatic activation as a cause of the difference in biological potency between MC and *ent*-MC.

Adducts of *ent*-MC and DNA. The strategy of adduct structure determination had to take into account the very limited

(25) Johnson, W. S.; He, Q.-Y.; Tomasz, M. *Bioorg. Med. Chem.* **1995**, *3*, 851−860.

(26) Pan, S.-S.; Pedersen, L.; Bachur, N. R. *Mol. Pharmacol.* **1981**, *19*, 184−186.

Scheme 3. Hydrolytic Loss of Deoxyribose in Mitomycin C– and *ent*-Mitomycin C–Deoxyguanosine Adducts upon N^7-Methylation of the Guanine Residue

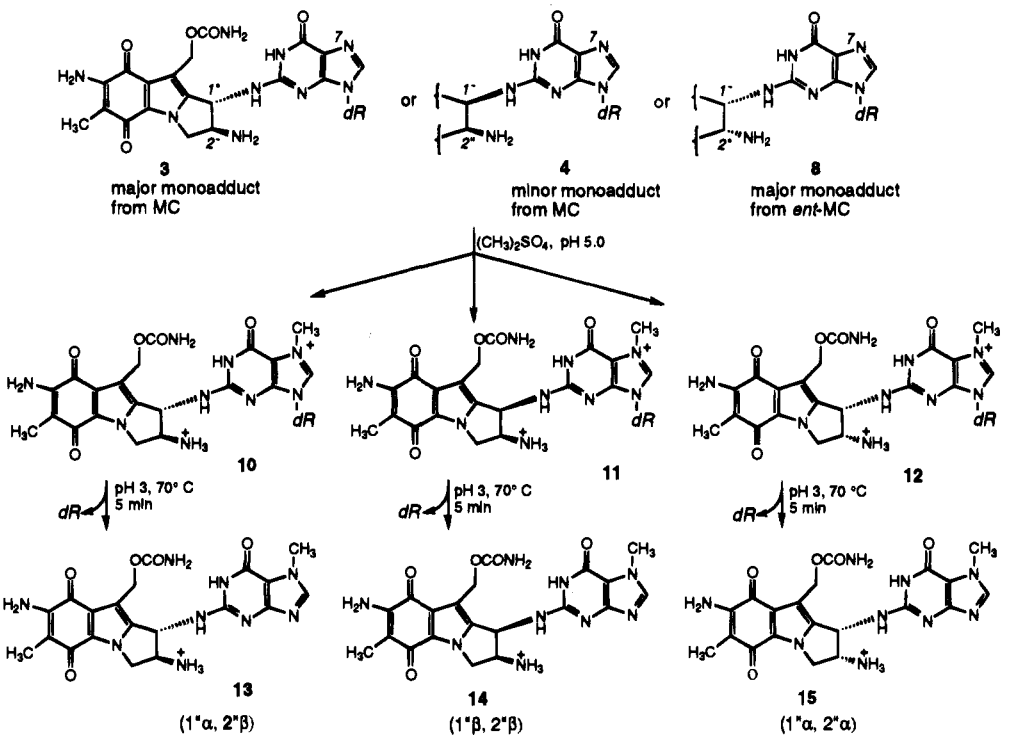

quantity obtained of these substances. The starting material *ent*-MC (**2**) was synthesized by Fukuyama and his co-workers,[8,9] but only 8 mg was available for this investigation. The amounts of isolated, pure DNA adducts never exceeded 150 μg. Use of ^{1}H NMR was not promising since mitomycin adducts need to be acetylated to give sharp NMR spectra[11a,b] and such procedures further diminish the quantity of the sample. Instead, we succeeded in assigning the structure of the unknown adduct of *ent*-MC as **8** by showing that it is the diastereomer of the known monoadduct of MC, **3**, based purely on optical spectroscopy (UV and CD) and mass spectral measurements of **8** and **3** and their chemical derivatives. Both of these methods required only microgram quantities of material. The usefulness of CD spectra in assigning the stereochemistry of mitosenes has been well proven in our previous studies.[11,22]

The putative cross-link (bisadduct **9**) was shown to be formed directly from the oligonucleotide-linked monoadduct **8** upon

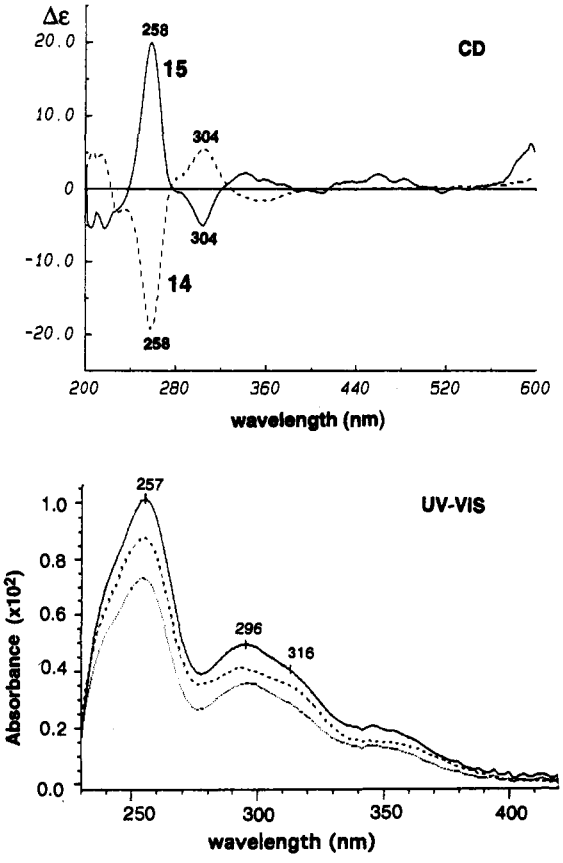

Figure 10. Top: CD spectra in water of the guanine N^7-methylated monoadducts **14** (dashed line) and **15** (solid line). Bottom: UV–vis spectra in water of deribosylated monoadducts **13** (dotted line), **14** (dashed line), and **15** (solid line).

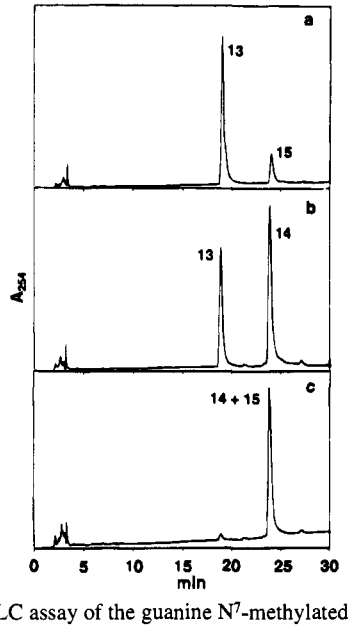

Figure 11. HPLC assay of the guanine N^7-methylated compounds **13**, **14**, and **15**. Coinjections of **13** and **15** (a) and **13** and **14** (b) show two distinct peaks because of their diastereomeric relations; coinjection of **14** and **15** shows only one peak because they are enantiomers. HPLC conditions: as in Figure 5.

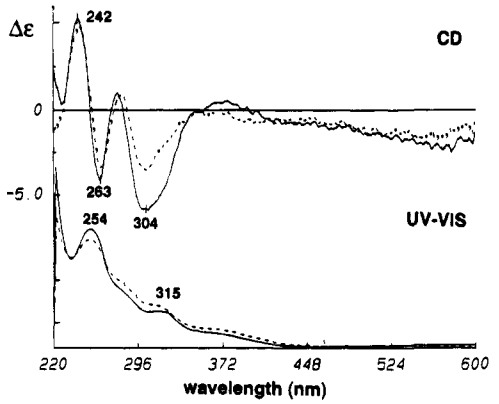

Figure 12. CD and UV−vis spectra in water of bisadducts **6** (solid line) and **9** (dashed line).

Scheme 4. Conversion of *ent*-MC-Monoalkylated Oligonucleotide **23** to *ent*-MC Cross-Linked Duplex Oligonucleotide **20**

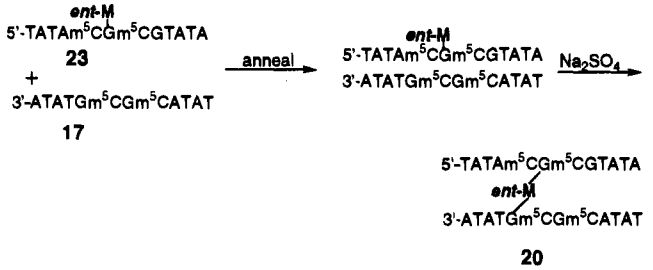

reduction (Scheme 4). This fact, together with the UV, mass, and CD spectra, serves as unequivocal proof of the structure of the bisadduct as **9**. Again, only microgram quantities were required for these determinations.

Significance of the Observed Stereochemistry of the *ent*-MC Adducts for the Mechanism of the Reaction of the Mitomycins with DNA. The adduct structures indicate that the two MC enantiomers react in a similar manner with DNA. This is not surprising considering that the different chirality of the original molecules is largely lost upon their reductive activation. The number of chiral centers in **1** and **2** is reduced from four to only one (the 2″-carbon) in the quinone methide forms **Red 5** and **Red 8** (Scheme 2). Since both major monoadducts **3** and **8** are C1″-α-linked to the DNA, it is apparent that DNA attacks both mitomycin enantiomers preferentially on their α-face even though this leads to a 1″,2″-*trans*-product (**3**) from MC and a 1″,2″-*cis*-product (**8**) from *ent*-MC. In contrast, the same reaction of MC *with monomeric deoxyguanosine* gives an equal amount of C1″-α- and C1″-β-adducts **3** and **4**.[27] The observed stereoselectivity of the reaction with duplex DNA can only be explained if one assumes that *prior to covalent bond formation* the two active mitomycin quinone methides **Red 5** and **Red 8** bind to DNA in a common, specific orientation relative to the target guanine in the chiral minor groove of the DNA, which determines a stereospecific attack by the guanine on the α-face of the mitomycins. The opposite chirality of the 2″-NH_2 group in the two agents does not perturb this orientation. This noncovalent association of the quinone methides with the chiral DNA renders their C1″-position prochiral; consequently, their covalent reaction with the target guanine at this prochiral center is stereospecific, yielding *the C1″-α-adduct* in both cases. This is not unlike the stereospecific reaction of an enzyme-bound prochiral substrate under enzymatic catalysis.[28]

(27) Tomasz, M.; Lipman, R.; Verdine, G. L.; Nakanishi, K. *Biochemistry* **1986**, *25*, 4337−4343.

(28) Stryer, L. S. *Biochemistry*, 3rd ed.; W. H. Freeman: New York, 1988; pp 385−386.

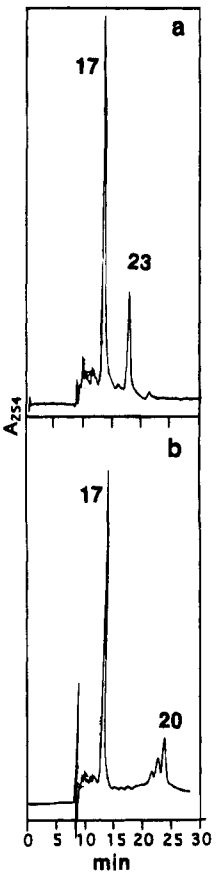

Figure 13. Conversion of monofunctionally bound *ent*-MC to a cross-link adduct upon reactivation by $Na_2S_2O_4$ in complex **23** (Scheme 4). HPLC analysis (a) before and (b) after $Na_2S_2O_4$ reactivation. HPLC conditions: column as in Figure 4; 7.5−9% CH_3CN in 0.1 M TEAA, pH 7.0, in 20 min, followed by 9−18% CH_3CN in 0.1 M TEAA, pH 7.0, in 20 min; the column was heated at 50 °C to improve the resolution.

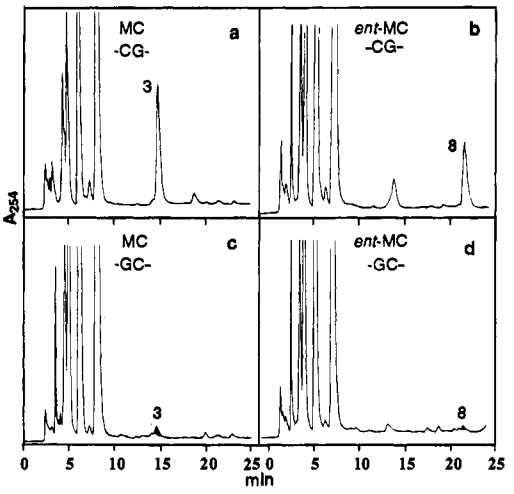

Figure 14. Monoalkylation specificity at the 5′-CG *vs* the 5′-GC site by MC and *ent*-MC. (a) Digest of reaction mixture **16b** and MC. (b) Digest of reaction mixture **16b** and *ent*-MC. (c) Digest of reaction mixture **25b** and MC. (d) Digest of mixture **25b** and *ent*-MC. HPLC conditions: as in Figure 5.

What structural factor(s) determine the precovalent orientation of the mitomycins in their complex with DNA? To analyze this, one should first consider that formation of the major C1″-α-MC−DNA monoadduct (**3**) is greatly enhanced at the CpG•CpG sequence in comparison to any other NpG•CpN′ sequence.[18] In contrast, the minor C1″-β-adduct of MC (**4**) in which DNA attack occurred on the β-stereoface is formed in similar, low yields atall NpG•CpN′ sequences, including

Table 1. Yields of Cross-Linking and Monoalkylation Products of *ent*-MC and MC with Various Substrates

	cross-linking yield (%)			monoadduct yield (%)		
drug	**16a**	**25a**	pBR322 DNA	**16b**	**17**	**16a**
MC	38	0	56,[a] 43[b]	78	68	24
ent-MC	7	0	27,[a] 12[b]	25	30	5

[a] At 20 μM drug concentration; see Figure 3. [b] At 10 μM drug concentration; see Figure 3.

Table 2. Growth-Inhibitory Activity of *ent*-Mitomycin C against Human Uterine Cervix Carcinoma HeLa Sa Cells[a,b]

	IC_{50} (μM)	
compound	1 h exposure time	72 h exposure time
MC	1.03	0.060
ent-MC	2.22	0.11

[a] Data from a personal communication by K. Gomi, Kyowa Hakko Kogyo Co., Tokyo, Japan. [b] The neutral red dye uptake method was described by Morimoto et al.[35]

CpG•CpG. The magnitude of these yields is about the same as that of the *major adduct 3 at its nonfavorable (non-CpG) target sequences*.[18b,29] This minor, β-adduct (**4**) is likely to be derived from the opposite, "carbamate downstream" orientation of the MC−guanine (Figure 15b). Thus, it appears that the two alternative precovalent orientations of the quinone methide **Red 5** (Figure 15; left side diagrams) are equally probable in the DNA minor groove, except at the CpG•CpG sequence where the "carbamate upstream" orientation is specifically promoted relative to the carbamate downstream orientation. A structural factor determining this specificity has been identified as a H-bond formed between the C10″-oxygen atom of the MC C10″-carbamate and the guanine 2-amino group in the nonbonding strand at the CpG•CpG duplex target site (Figure 15a).[15,18b,c,30b] On the basis of the magnitude of the increased yield of formation of **3** at this sequence relative to that at the other sequences, it was concluded that not only the noncovalent carbamate upstream orientation ratio but also the *rate of formation of the covalent monoadduct* **3** was increased at this sequence.[18b] The rate increase was similarly attributed[18b] to the specific H-bond, in accordance with the general concept of increased reactivity of bound complexes.[31,32] It is inherent in this mechanism that once the mitomycin is *covalently* linked as the C1″-α-monoadduct, its carbamate upstream orientation is irreversibly fixed; i.e., the C1″-α-monoadduct should spontaneously orient itself this way when the adducted duplex is denatured and then reannealed. This predicted property was explicitly demonstrated in the case of MC by a recent NMR study of the solution structure of a duplex oligonucleotide containing a C1″-α-monoadducted CpG•CpG site.[15] This duplex was shown to exist solely as the carbamate upstream orientation isomer. Furthermore, although the structure clearly revealed the postulated specific H-bond, this H-bond was not a *necessary* determinant of the orientation in the *covalent* complex. This was dramatically demonstrated by comparison of the NMR of the monoadducted duplex in which the unsubstituted complementary strand was replaced by a strand containing CpI instead of CpG. This duplex retained the single carbamate upstream orientation of the monoadduct even though the specific H-bond was not possible at its CpG•CpI sequence (cf. Figure 15a).[15] Thus, the structural origin of the specific orientation of the major, C1″-α-monoadduct **3** in the minor groove does not reside in the carbamate H-bond, as in the precovalent stage, but rather in the α-chirality of the covalent bond to DNA, which would now prevent a good fit of the drug in the opposite orientation. This is exactly as predicted by molecular mechanics-based modeling by Hopkins and co-workers[17] and, less directly, by Arora *et al.*[30a]

ent-MC served as an independent probe for the validity of this mechanism. Its major adduct showed the same precovalent orientation specificity, the same CpG-sequence selectivity, *and* the same DNA-bond chirality as MC's major adduct. Since the specific structural features of the MC adduct assigned to be responsible for the mechanism are also the same in the *ent*-MC adduct, these assignments (that is, the mechanism) are probably correct.

It is interesting that the α-monoadducts of MC and *ent*-MC conform to an empirical relationship in the class of minor groove monoalkylators: the chirality of their connection to DNA determines a specific orientation in the minor groove. Thus, the (+)- and (−)-CC-1065 enantiomers form α- and β-connections with DNA, respectively, and lie in opposite orientations.[5a] Adducts of CC-1065 analog enantiomer pairs[5b] as well as those of duocarmycin SA enantiomers[5c] and BPDE enantiomers[7a,b] and C11-(*S*)-adducts of anthramycin[33a,b] and tomaymicin[33c] follow this pattern. In the present case, both mitomycin enantiomers form α-bonds with DNA as major adducts, and correspondingly, both lie in the *same* orientation.

The slightly but consistently lower yields of the *ent*-monoadduct **8** and its derivative bisadduct **9** compared to the MC monoadduct **3** and bisadduct **6** (Table 1) indicate that the reaction of *ent*-MC with DNA is less favorable overall. It is likely that the 2″-α-amino group, originating from the α-aziridine stereochemistry of *ent*-MC (**2**) lowers the stability of the precovalent complex (Figure 15a) due to a slightly less favorable fit for covalent reaction. Modeling experiments should be able to critically test this hypothesis.

As another important outcome of this study, the observed C1″-α-linkage of the major adducts to DNA from both MC enantiomers serves as striking confirmation of the earlier notion that DNA alkylation by activated MC proceeds by an S_N1 attack on the quinone methide **Red 5**[34] rather than S_N2 attack on the aziridine form, **Red 4** (Scheme 2). The latter mechanism would lead to opposite C1″-stereochemistries of the major adducts of MC and *ent*-MC which is not the case.

***ent*-MC Adducts and Biological Activity.** Remarkably, *ent*-MC has a cytotoxic potency similar to that of MC.[19] It is gratifying that we could correlate this with a similarity of their action on DNA. On the basis of the single set of available biological data, *ent*-MC appears to have slightly lower (0.5-fold) cytotoxic potency than MC, nevertheless (Table 2). One may speculate that this is due to its lesser (0.3−0.5-fold) capacity to induce monoalkylation and cross-linking damage in DNA, as observed here (Table 1). This lesser capacity may be due to a slight steric hindrance to the reaction by the 2″-α-amino group of the activated *ent*-MC.

Summary. *ent*-MC forms 1″-α-linked monoadducts and bisadducts with DNA as the major products upon reductive

(29) Unpublished results from this laboratory.

(30) (a) Arora, S. K.; Cox, M. B.; Arjunan, P. *J. Med. Chem.* **1990**, *33*, 300−3008. (b) Remers, W. A.; Rao, S. N.; Wunz, T. P.; Kollmann, P.; *J. Med. Chem.* **1988**, *31*, 1612−1620.

(31) Menger, F. M. *Acc. Chem. Res.* **1985**, *18*, 128−134.

(32) The specific H-bond under discussion is not the only binding element in the complex; nevertheless, it is *additional* to the other, nonspecific ones.[30b]

(33) (a) Krugh, T. R.; Graves, D. E.; Stone, M. P. *Biochemistry* **1989**, *28*, 9988−9994. (b) Boyd, F. L.; Cheatham, S. F.; Remers, W. A.; Hill, G. C.; Hurley, L. H. *J. Am. Chem. Soc.* **1990**, *112*, 3279−3289. (c) Boyd, F. L.; Stewart, D.; Remers, W. A.; Barkley, M. D.; Hurley, L. H. *Biochemistry* **1990**, *29*, 2387−2403.

(34) (a) Moore, H. W. *Science* **1977**, *197*, 527−532. (b) Tomasz, M.; Lipman, R. *Biochemistry* **1981**, *20*, 5056−5061. (c) Peterson, D. M.; Fisher, J. *Biochemistry* **1986**, *25*, 4077−4084. (d) Schiltz, P.; Kohn, H. *J. Am. Chem. Soc.* **1993**, *115*, 10510−10518.

(35) Morimoto, M.; Ashizawa, T.; Ohno, H.; Azuma, M.; Kobayashi, E.; Okabe, M.; Gomi, K.; Kono, M.; Saitoh, Y.; Kanda, Y.; Arai, H.; Sato, A.; Kasai, M.; Tsuruo, T. *Cancer Res.* **1991**, *51*, 110−115.

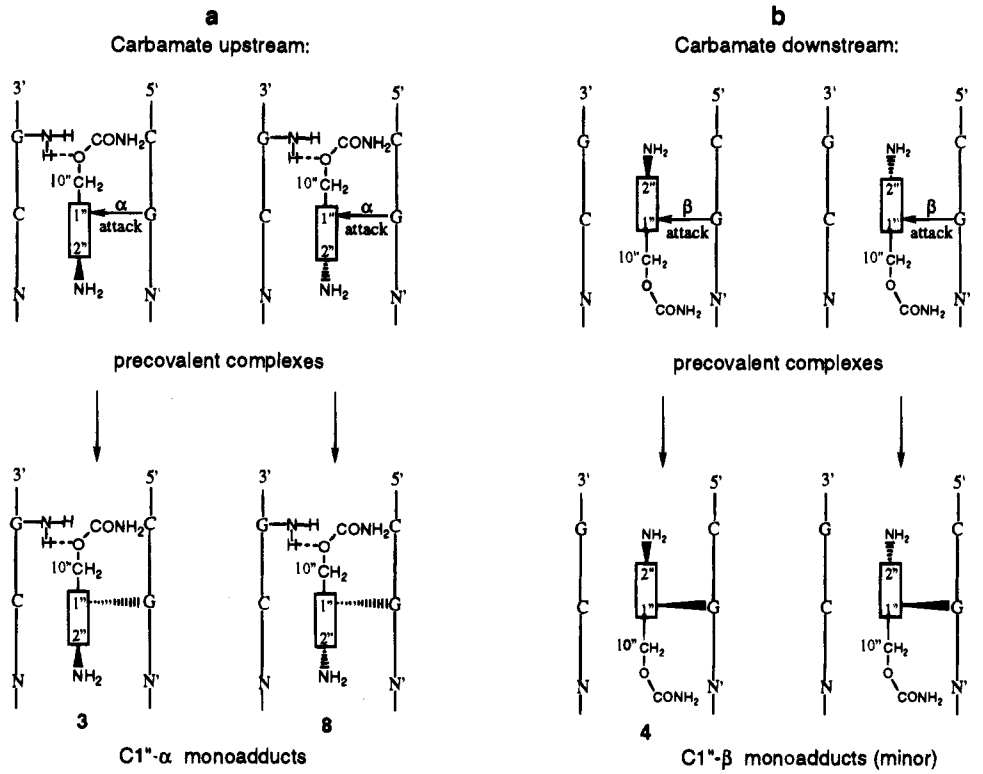

Figure 15. Orientation of the quinone methide form of the mitomycins in the precovalent complex determines the stereochemistry of the monoadduct–DNA covalent bond. In both sets (a) and (b) MC and *ent*-MC are depicted on the left and on the right, respectively.

activation. The stereochemistry of the drug–DNA linkage is thus the same as with MC despite the opposite stereochemistry of the aziridine of the two mitomycin C enantiomers. The mechanism of the α-attack by DNA in both cases is determined by the common precovalent orientation of the two mitomycin active forms relative to the target guanine in the minor groove; this orientation is stabilized relative to the opposite one by a H-bond interaction between the 10″-carbamate of the drug and DNA, specifically at CpG•CpG sequences. The binding also enhances the rate of subsequent covalent bond formation. The 2″-α-amino group of the *ent*-MC form may cause a slight steric hindrance to this alignment in the precovalent drug–DNA complex, unlike the 2″-β-amino group of the natural mitomycin, which is more favorably positioned. This difference could account for the observed lower yields of DNA adducts with *ent*-MC than with MC.

Experimental Section

Materials. *M. luteus* DNA was obtained from Sigma, St. Louis, MO, and was sonicated before use. Oligonucleotides were synthesized on an automated DNA synthesizer (model 380B, Applied Biosystems, Inc.), using the β-cyanoethyl phosphoramidite method. All necessary reagents were purchased from Applied Biosystems Inc., Foster City, CA. The crude products (1 μmol scale, "trityl off"), after deprotection by concentrated NH_4OH overnight at 55 °C, were purified using a Sephadex G-25 (fine) column (2.5 × 56 cm; 0.02 M NH_4HCO_3 eluant). The void volume fractions, containing the oligonucleotide, were lyophilized. HPLC on a semipreparative C-4 column (see below) indicated ≥95% purity of the oligonucleotides.

Mitomycin C (bulk) was supplied by Bristol-Myers Squibb Co., Wallingford, CT. *ent*-MC was prepared in the laboratory of Dr. T. Fukuyama, as described in the Ph.D. thesis of L. Yang.[8]

DNase I (code D), phosphodiesterase I (snake venom diasterase) and *Escherichia coli* alkaline phosphatase (type III-R) were purchased from Worthington, Freehold, NJ. NADPH–cytochrome *c* reductase was a gift from Dr. Wayne Backes (Louisiana State Medical School, New Orleans, LA). NADPH was purchased from Sigma. Dimethyl sulfate was purchased from Aldrich.

Methods. Quantities of oligonucleotides were measured by UV spectrophotometry and are expressed in moles of mononucleotide units. One A_{260} unit of oligonucleotide corresponds to 0.1 μmol of mononucleotide units, based on an average E_{260} = 10 000 per mononucleotide unit. The percent yield of cross-linked oligonucleotides **18** and **19** was calculated from the areas of the parent and cross-linked duplex peaks in the HPLC pattern (cf. Figure 5), as follows: % yield of cross-linked oligomer = 100(area of cross-linked oligomer/area of parent oligomer). The percent yields of monoadducts **3**, **4**, and **8** present in the enzymatic digest of oligonucleotides alkylated by MC and *ent*-MC were calculated according to a published procedure.[18b] The percent yields of methylation of monoadducts **3**, **4**, and **8** to give **10**, **11**, and **12** were calculated from the ratio between the areas of the peaks corresponding to products and to starting materials, respectively, in the HPLC pattern. The same procedure was used to calculate the percent yield of deribosylated adducts **13**, **14**, and **15** from **10**, **11**, and **12**.

Spectroscopic Techniques. The UV spectra were recorded on a Perkin-Elmer Lambda 4B UV–vis spectrophotometer; the CD spectra were recorded on a Jasco 720 spectropolarimeter. The following extinction coefficient values (E) were employed to determine the concentration of the adducts from the UV–vis spectra: E_{252} = 24 000 for monoadducts **3**, **4**, and **8**; E_{252} = 30 000 for bisadducts **6** and **9**; E_{312} = 10 590 for deribosylated monoadducts **13**, **14**, and **15**.

LC–MS data were obtained on a Finnigan (San Jose, CA) Model 4500 spectrometer with a Vestec electrospray ion source. A Hewlett-Packard Model 1050 HPLC pump provided a flow rate of 200 μL/min through a YMC, Inc., C-18 AQ column (25 cm × 2.0 mm, 5 μm particles). A linear gradient of 5–30% CH_3CN in 0.1% CH_3COOH in 30 min was used for the separations. The effluent from the HPLC column was split 15:1, with 187 μL/min directed to the UV detector (312 nm) and 13 μL/min directed to the electrospray ion source. Sulfur hexafluoride was used as the nebulizing gas, and a needle voltage of 4 kV was used to effect ionization. The mass spectrophotometer was controlled with a Teknivent (Maryland Heights, MO) Vector 2 data system which scanned the instrument from 130 to 650 amu at a rate of 2 s/scan.

HPLC. A Beckman System Gold 125 instrument, equipped with a diode array detector System Gold 165, and controlled by System Gold Chromatography Software, was used.

Reduction Kinetics of MC and *ent*-MC. NADPH–cytochrome *c* reductase-catalyzed reduction of MC and *ent*-MC was monitored by

HPLC, following the conversion of the starting material to mitosene-type quinones. To a deaerated solution containing 0.45 mM MC or *ent*-MC, 0.52 mM NADPH, and 0.45 mM thymidine as the internal HPLC standard in 300 μL of 0.1 M Tris buffer (pH 7.4) was added NADPH−cytochrome *c* reductase (2.5 units/μmol of drug). The reaction flask was incubated at 37 °C under positive pressure of helium to ensure anaerobic conditions. Twenty-five microliter aliqots of the reaction mixture were taken and diluted to 50 μL with methanol at 0, 2.5, 5, 10, 15, 20, 30, and 40 min after the addition of the enzyme. HPLC of the reaction mixtures was conducted using a C18 analytical column and 0−18% CH_3CN in 0.02 M NH_4OAc, pH 5.2, in 40 min, as the elution gradient. The extent of MC (or *ent*-MC) reduced was calculated from the areas of the appropriate HPLC peaks as follows:

$$\%\ \text{MC reduced} = 100 - \frac{[\text{area of MC/area of dT}] \times 100}{[\text{area of MC/area of dT}]_{0\ \text{time}}}$$

Cross-Linking of Oligonucleotides 16a by *ent*-MC To Give 18. Our standard procedure of cross-linking of oligonucleotides by MC was employed.[12] This consisted of incubating *ent*-MC, duplex oligonucleotide, and $Na_2S_2O_4$ as the reductive agent in neutral aqueous buffer at 0 °C under anaerobic conditions. The reaction was conducted using 0.1 μmol of **16a** and 0.4 μmol of *ent*-MC in a total reaction volume of 50 μL. The yield of the cross-linked oligonucleotide was 7% as calculated from HPLC analysis (Figure 4). The same procedure was applied using another oligonucleotide **25a**, as the substrate. In this case no cross-linked oligonucleotide was formed as seen by HPLC (Figure 4c).

Isolation of a "Cross-Link" Adduct (9) from Enzymatic Digests of the Cross-Linked Oligonucleotide 18. Oligonaucleotide **18** was digested to nucleotide level by SVD and alkaline phosphatase in combination. In a typical procedure, 1 A_{260} unit/mL of drug−oligonucleotide adduct in 200 μL of 0.1 M Tris/2 mM $MgCl_2$, pH 8.2, was incubated for 1 h at 45 °C, in the presence of SVD (1 unit/A_{260} unit) and alkaline phosphatase (0.7 unit/A_{260} unit). The resultant digested mixture was analyzed by HPLC, and the adduct **9** was isolated by collecting the HPLC peak (Figure 7): MS *m/z* (relative intensity) 776 (M+, 100); UV−vis (H_2O) λ_{max} 253, 313, 353, 553 nm (Figure 9).

Monoalkylation of Oligonucleotides 16b and 17 by *ent*-MC under Reductive Activation to Give 21 and 23, respectively. A mixture of self-complementary oligonucleotide **16b** or **17** (1 mM in mononucleotide unit) and *ent*-MC (2.5 mM) in 0.1 M sodium phosphate buffer, pH 7.4, in the presence of PtO_2 as a catalyst (ca. 100 μg/μmol of drug) was deareated at room temperature with helium. Hydrogenation was carried out for 4 min followed by helium purge before opening to air. PtO_2 was removed *via* filtration. Monoadducted oligonucleotides **21** and **23** were each isolated together with their unmodified parent oligonucleotide, using a 2.5 × 56 cm Sephadex G-25 column and 0.02 M NH_4HCO_3, pH 8.1, as eluant. The yields of monoadduct oligonucleotides **21** and **23** were 25% and 30%, respectively, as determined by HPLC analysis of monoadduct **8** in the digests of the reaction mixtures (see Figure 7b for the HPLC analysis).

Isolation of Monoadduct 8 from Enzymatic Digests of Monoalkylated Oligonucleotides 21 and 23. This was accomplished following the same enzymatic digestion procedure using for the bisadduct derivative **9**. The monoadduct **8** was isolated by collection of the appropriate HPLC peak (Figure 7b): **8** MS *m/z* (relative intensity) 570 (MH^+, 75), 509 ($MH^+ - NH_3CO_2$, 48), 454 (MH^+ − dR, 15), 393 (509 − dR, 100), 376 (393 − NH_3, 32), 285 (MH^+/2, 88); Uv−vis (H_2O) λ_{max} 253, 313, 353, 553 nm.

Conversion of *ent*-MC-Monoadducted Oligonucleotide 23 to *ent*-MC-Cross-Linked Oligonucleotide 20 (Scheme 4). A mixture of monoadduct oligonucleotide **23** (0.7 A_{260} unit) and the unmodified oligonucleotide **17** (2.2 A_{260} units; 3-fold molar excess) in 600 μL of 0.1 M Tris, pH 7.4, was briefly heated at 50 °C, and then allowed to cool to 4 °C and deaerated with argon. Excess NaS_2O_4 (30 μL of a 0.042 M solution anaerobically prepared in the above buffer) was added at once. The solution was stirred under argon in an ice bath (4 °C) for 45 min and then opened to air and analyzed by HPLC. The results (Figure 13) show that **23** disappeared completely from the reaction mixture and **20** was formed, along with lesser amounts of unidentified products. The identity of **20** was verified by digestion of the collected HPLC peak to adduct **9** (cf. Figure 6b).

Methylation of Monoadducts 3, 4, and 8 to Give 10, 11, and 12 (Scheme 3). To a solution of monoadduct **3, 4**, or **8** (2.3 A_{254} units; 57 μg, 0.1 μmol) in 200 μL of cold 0.3 M potassium phosphate, pH 5.0, was added DMS (27 mg, 0.211 mmol), and the resulting mixture was stirred at room temperature for 2 h. The reaction was monitored by HPLC using the general conditions described above, by detecting the disappearance of the peak corresponding to the starting adduct, and the appearance of a new peak with shorter elution time, corresponding to the 7-methylated deoxyguanosine adducts **10**, **11**, and **12** (data not shown). These were isolated by HPLC from the original reaction mixture in more than 80% yield. Before proceeding to the subsequent step of deribosylation, the LC−MS of **10** and **11** was recorded. Due to the very limited amount of **12** available, its MS was recorded only after deribosylation. Data for **10**: MS *m/z* (relative intensity) 584 (M^+, 70); 469 (MH^+ − dR, 40); 407 (469 − NH_3CO_2, 100); UV−vis (H_2O) λ_{max} 257, 292, 317, 353 nm. Data for **11**: MS *m/z* 584 (M^+, 90); 523 ($M^+ - NH_3CO_2$, 20); 468 (M^+ − dR, 50); 407 (468 − NH_3, 100); 390 (407 − NH_3, 20); UV−vis (H_2O) λ_{max} 257, 292, 317, 353 nm.

Deribosylated Methylated Monoadducts, 13, 14, and 15 from 10, 11, and 12. Two A_{260} units were dissolved in 400 μL of water, the pH was adjusted to 3.0 with glacial acetic acid, and the samples were heated at 85 °C for 5 min. This treatment led to hydrolytic cleavage of the deoxyribose residue, to afford compounds **13**, **14**, and **15**. The reaction proceeded with an almost quantitative yield judging from the HPLC pattern (complete disappearance of starting material peak, appearance of new peak with later elution time). Data for **13**: MS *m/z* (relative intensity) 468 (M^+, 35), 407 ($M^+ - NH_3CO_2$, 100), 390 (407 − NH_3, 12), 242 (8); UV−vis (H_2O) λ_{max} 257, 296, 316, 353 nm (Figure 10). Data for **14**: MS *m/z* (relative intensity) 468 (M^+, 30), 407 ($M^+ - NH_3CO_2$, 100), 390 (NH_3, 18); UV−vis (H_2O) λ_{max} 257, 296, 316, 353 nm (Figure 3). Data for **15**: MS *m/z* (relative intensity) 468 (M^+, 20), 407 ($M^+ - NH_3CO_2$, 100), 390 (407 − NH_3, 40), 235 (M/2 + H^+, 30); UV−vis, same as above (Figure 10).

Monoalkylation Specificity at the 5′-CG *vs* the 5′-GC Site by MC and *ent*-MC. This was determined by alkylating oligonucleotides **16b** ("5′-CG site") and **25b** ("5′-GC site") by monofunctionally activated MC or *ent*-MC under identical conditions. The reaction mixtures were digested, and the yields of corresponding monoadducts were determined from HPLC tracing (Figure 14). We found that **16b** yielded 78% of monoadduct **3** with MC and 25% of monoadduct **8** with *ent*-MC. In contrast, **25b** yielded less than 5% of these adducts with the drugs, indicating clearly that monoalkylation favors the 5′-GC site, in the cases of both MC and *ent*-MC.

Acknowledgment. We thank Dr. Koji Nakanishi of Columbia University, New York, for allowing us to use his CD instrument, Dr. D. M. Vyas of Bristol-Myers Squibb Co., Wallingford, CT, for a generous gift of mitomycin C, Dr. Wayne Backes of Louisiana State Medical School, New Orleans, for NADPH−cytochrome *c* reductase and Dr. K. Gomi of Kyowa Hakko Kogyo Co., Tokyo, Japan, for permitting us to quote his unpublished results on the biological activity of *ent*-mitomycin C. The expert contribution of Dr. Qiao-Yun He to the pBR322 DNA cross-linking experiments is also acknowledged. This research was supported by a grant (CA28681) from the National Cancer Institute and a Research Centers in Minority Institutions award (RR003037) from the Division of Research Resources, NIH (both to M.T.), and by NIH Grant CA28119 (to T.F.).

JA951317F